Journal of Structural Geology. Vol. 4. No. 4. pp. 443 to 455. 1982
Printed in Great Britain

0191-8141/82/040443-12 $03.00/0

Domainal and fabric heterogeneities in the Cap de Creus quartz mylonites

A. GARCIA CELMA

Instituut voor Aardwetenschappen, Budapestlaan 4, 3584 CD Utrecht, Nederland

(*Received* 8 *May* 1981; *accepted in revised form* 20 *May* 1982)

Abstract—A characteristic domainal configuration is reported for both micro-structures and c-axis fabrics in the Cap de Creus pure quartz mylonites as displayed in 50 samples from the centres of different shear zones. Three types of domains are found *a*, *b* and *c*. Each domain has a distinct c-axis orientation pattern. These three fabric elements, also labelled *a*, *b* and *c* make up the total fabric. c-axis fabrics are symmetric or asymmetric with respect to the main mylonitic foliation depending on the presence or absence of the *b* domain and its fabric element. The boundaries of the domains are parallel to the main mylonitic foliation. Two domain types, *a* and *b* display an internal foliation defined by preferred grain boundary alignment parallel to the direction of optical orientation within the domain. The internal foliations are oblique to the main mylonitic foliation in two different senses giving the sample a herring-bone appearance. These internal foliations are shown to be related to extensional crenulations. Domains are not produced by host-controlled recrystallization. The fabric elements and corresponding domains are the expression of kinematic heterogeneities on the scale of the thin section.

INTRODUCTION

DOMAINAL microstructures have been described by Sander (1950) and Eisbacher (1970) and interpreted as the result of polygonization of large porphyroclasts. Ramsauer (in Sander 1950) defined fabric elements and related them however to crenulations of the main mylonitic foliation. Other workers have explained fabric variations in naturally deformed quartzites in terms of heterogeneities of the deformation. Bouchez (1977) and Mancktelow (1981) showed how grains acquired different deformation-induced microstructures, c-axis fabrics and deformed shapes depending on their initial crystallographic orientation. Lister & Price (1978) related domainal heterogeneities and c-axis fabrics to variation of strains around feldspar clasts.

Two coexisting foliations, one being the mesoscopically visible mylonitic foliation and the other constituted by grain shape preferred orientation, were described by Brunel (1980) who interpreted them as products of different deformation events. Means (1981) pointed to the possible existence of both foliations as the result of simple shear deformation.

Etchecopar (1974, 1977), by means of computer simulations, produced both foliation and domainal microstructure by simple shear. The 'grains' in his model were simulated by cells which maintained their areas throughout deformation. In this model, grain size is essentially constant and the production of domains and preferred grain boundary alignment is due to 'fabric memory' and strain compatibility constraints between adjacent grains. The dependence of a fabric on the deformation path and the original orientation of its elements is referred to as 'fabric memory' (Lister & Price 1978).

This paper describes correlations which exist between microstructural domains, grain-boundary alignment foliations and crystallographic fabrics in quartz mylonites which are found in the central part of shear zones in the Cap de Creus area, Gerona Province, Spain. Introduction to the geology of the area can be found in Carreras (1973, 1974, 1975a, b), Carreras & Santanach (1973) and Carreras *et al.* (1977). The Cap de Creus area constitutes the most eastern outcrop of the axial zone of the Pyrenees. Many shear zones cutting through cordierite–andalusite grade schists outcrop in the northern area of the Cap de Creus. Almost pure quartzite nodules and veins occur in the schists. The schists are retrograded to greenschists-facies phyllonites in the shear zones and thus the shearing is inferred to have occurred under greenschist-facies conditions (Carreras *et al.* 1977). The schists are sheared together with the quartz nodules and veins from which the samples described here were collected. All the microstructures and c-axis fabrics described vary consistently with the shear zone geometry and are considered to have developed by bulk simple shear (Carreras *et al.* 1977).

The shear zones are characterized by a progressive rotation of the axial-plane schistosity of pre-existing folds towards parallelism with the shear-zone boundary (Carreras 1973, 1974). This schistosity will be here referred to as the regional schistosity (S), and where this foliation is parallel to the boundaries of the shear zone (mylonite zone) it is also called the main mylonitic foliation (Sm). In many shear zones there is no interruption of foliation planes which grade continuously from regional schistosity (S) to main mylonitic foliation (Sm). The main mylonitic foliation is almost coincident with the XY plane of the finite strain ellipsoid and X corresponds to the stretching lineation (L) and approximately to the direction of movement (Carreras & Santanach 1973).

Extensional crenulation cleavages (S_1 and S_2) which are only found in the shear zones are the subject of recent research with Carreras. They are shown to have constant orientation relationships with the regional

schistosity in the shear zone, turning congruently with it as the regional schistosity approaches the shear zone boundary (*Sm*).

Thin sections were cut perpendicular to the mylonitic foliation, *Sm*, and/or regional schistosity, *S*, and parallel or perpendicular to the stretching lineation, *L*. The sense of shear was deduced from field observations. The samples were classified into three types. Type I samples were taken from the boundaries of the shear zones where the regional schistosity makes a large angle to the shear zone boundary. Type III samples came from the centres of the shear zones where the regional schistosity (here the mylonitic foliation) is nearly parallel to the mylonitic boundary. Type II samples were from intermediate positions between type I and type III.

A resumé of the microstructures corresponding to types I, II and III will be given here before describing the domain microstructure which occurs in type III samples. The relationships between quartz porphyroclasts and recrystallized grains are described in order to analyse the origin of the domain microstructures. The changes in domainal microstructures around rigid crystals and the relationships between domains and mesoscopically visible foliations (*Sm*, S_1 and S_2) are also analysed and consideration is given to the kinematical significance of domain microstructures.

THE MICROSTRUCTURES

The angular relationships between the regional schistosity and the shear zone boundaries are used to indicate the finite strain of the samples.

The least deformed samples (type I)

Samples of quartzite collected from parts of the shear zones in which the regional schistosity is only slightly bent by the shear, belong to this group. In hand specimens, the quartzite is normally unfoliated. An incipient foliation and lineation develops towards the centre of the shear zone, but samples displaying a good foliation and stretching lineation are assigned to type II.

Under the microscope, samples from type I are constituted by irregularly shaped porphyroclasts from 5 to 10 mm in diameter showing deformation bands and undulose extinctions. Smaller grains of 100 μm in size occur at grain boundaries and along the most misoriented deformation bands of the megacrysts. The volume percentage of small grains (matrix grains) increases with deformation from 7 to 25% or more. Matrix grains do not display any preferred dimensional orientation.

Intermediate deformed samples (type II)

These samples were collected nearer to the centre of the shear zones than those corresponding to type I. The angle of the regional schistosity with the mylonitic boundary is appreciable, but smaller than the corresponding angle in type I. Type II samples in contrast to those of type I display a well developed foliation and stretching lineation.

Type II samples have a larger proportion of small grains than those corresponding to type I, so that as the angle between the regional schistosity and the shear zone boundary diminishes the volume ratio of small grains to porphyroclasts increases from 25 to 85%. The porphyroclasts are oblate to prolate in shape and their axes tend to be parallel to the regional schistosity whatever the angle between the regional schistosity and the mylonitic boundary. The most prominent deformation-induced microstructures in the porphyroclasts are the deformation bands which tend to be parallel to the porphyroclast boundaries and regional schistosity. In many porphyroclasts occurring in the most deformed samples of this type, the deformation bands can be described as kink bands. Internal to the deformation bands, smaller subgrains with boundaries oblique to the main deformation band boundaries exist. The orientation of the smaller subgrains depends on the crystal orientation. This internal microstructure of the deformation bands seems to continue into the matrix grains at their boundaries. The matrix constituted by the small grains acquires an incipient domainal distribution. All these microstructures are progressively more pronounced as the angle between the regional schistosity and the mylonitic boundary diminishes.

Highly deformed samples (type III)

Samples of quartzite occurring in the centres of the shear zones show a very penetrative mylonitic foliation and stretching lineation (*L*). Type III samples are the most deformed samples of each sequence; they are almost exclusively composed of matrix grains which constitute from 85 to 100% of the volume of the specimens. Some remnant porphyroclasts, most of them prolate, but also oblate and rarely globular, are present. Many of the matrix grains show deformation lamellae and/or extinction bands, preferred crystallographic orientations and preferred grain-boundary alignment, which define directions that can be followed into the porphyroclasts. These directions vary from domain to domain and characterize them. Their features and relationships will be described later.

Porphyroclast–matrix grain relationships

The similarity of size and shape of subgrains in the porphyroclasts and matrix grains, and the core-mantle microstructure of the samples, points to an origin by polygonization recrystallization (White 1976) of the latter. The c-axes of recrystallized grains are oriented near the host c-axis and their crystallographic orientation, according to Carreras *et al.* (1977), reflects the influence of host control in the less deformed samples (type I and incipient type II). However, it seems that such coincidence in c-axis orientation is better described as fabric memory. Figures 1(a) and (b) and Figs. 1 (c)

and (d) show the c-axis fabrics of two samples from the same quartz lens, but corresponding to type I and II, respectively. Although the orientation of porphyroclasts is related to the recrystallized grains situated within them, the angular spread of c-axes from all new grains is not centred around the orientation of the c-axes of the porphyroclasts but gives rise to the pseudo-two-girdle fabric distribution which is the stable c-axes fabric for Cap de Creus for moderate simple shear deformations. Note that the trends of spreading of subgrain orientation of porphyroclasts (Figs. 1a & c) are different from the patterns of new grains (Figs. 1b & d); for instance old grain c-axes occupy empty areas on the new grain fabric diagram. This argues against the operation of host control. Moreover, the recrystallized grain c-axis fabric of a type I sample (Fig. 1b) fits better to a pseudo-two-girdle pattern than the porphyroclasts of a type II sample (Fig. 1c) which is more deformed. In the type II sample (Figs. 1c & d) the porphyroclasts have not adapted as a whole to a pseudo-two-girdle fabric, while the new grains develop a fabric which already shows an incipient asymmetry. Hence, although recrystallized grains 'remember' the porphyroclast orientation, their c-axis fabric is determined by deformation rather than host control, and recrystallization reinforces the fabric.

Grain sizes and grain boundaries

Accompanying increasing deformation and fabric development, the mean grain size decreases as a consequence of polygonization of porphyroclasts. The grain size of matrix grains is homogeneous on the scale of a thin section, except for those specimens containing mica-rich layers. On a larger scale, the grain size of matrix grains from the centres of different shear zones

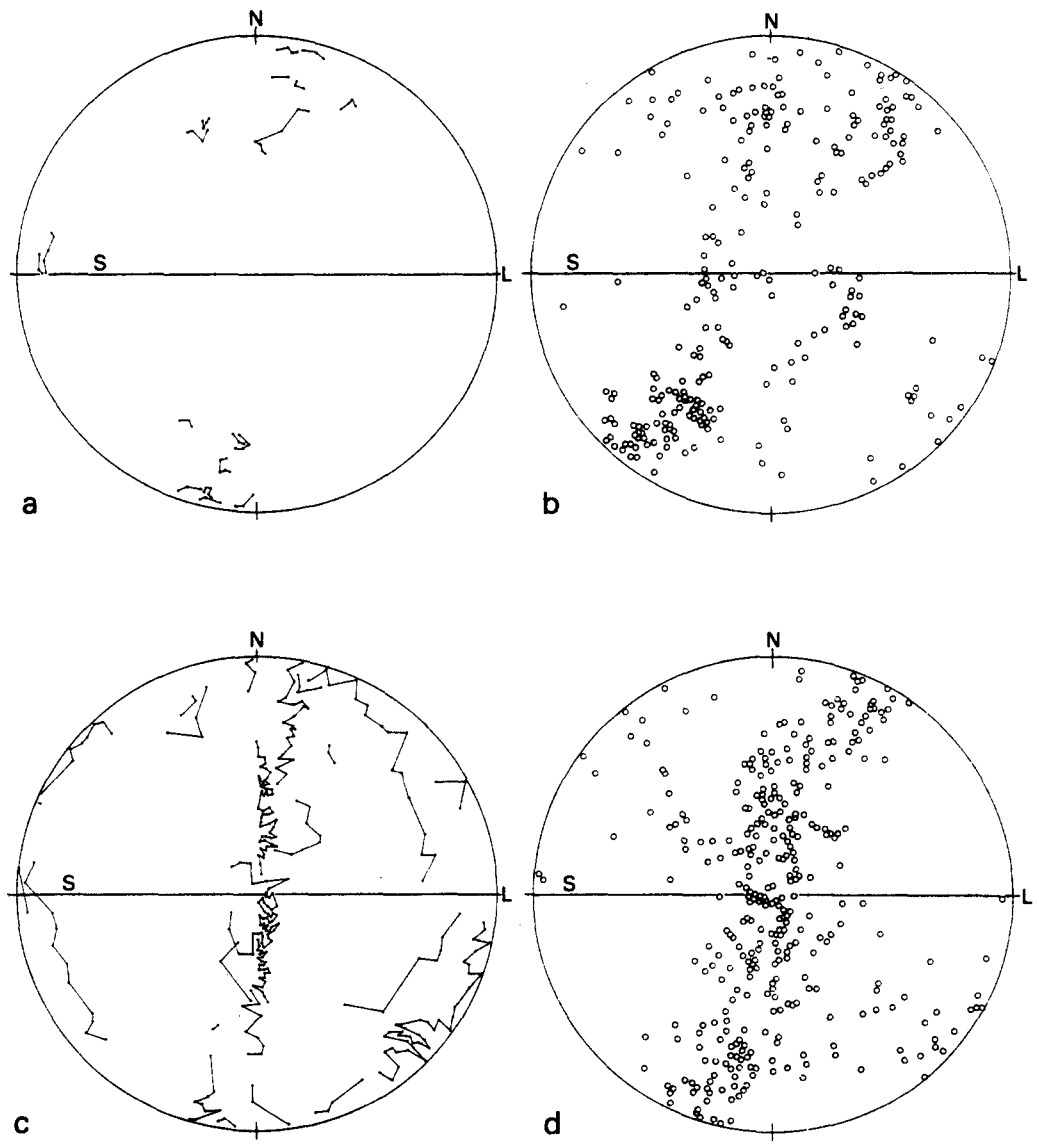

Fig. 1. Relationships between porphyroclast and recrystallized grain c-axes orientations. (a) Subgrain c-axes plots of porphyroclasts from a type I sample. (b) New grain c-axis fabric from the same specimen as (a). (c) Subgrain c-axes plots of porphyroclasts from a type II sample belonging to the same shear zone as (a) and (b). (d) New grain c-axis fabric from the same specimen as (c). In (a) and (c) the subgrain c-axes plots from the same porphyroclast are joined by lines. Only one of each similar porphyroclast trend of spreading is represented. Note that old grain populations from (a) and (c) differ more than the new grain fabrics from the same specimens (b and d). (S regional schistosity, N its pole, L lineation).

varies from one sample to another within the range of 100 μm and 20 μm. However, differences in the grain sizes of the matrix grains between different samples from the centres of different shear zones do not correlate with the c-axis fabric characteristics. The grain boundaries of recrystallized grains are generally straight whilst grain boundaries of porphyroclasts are serrated.

THE DOMAINS

Within type III samples, recrystallized grains with similar lattice orientation patterns are arranged in domains parallel to the main mylonitic foliation (*Sm*). The microstructure of the rock varies consistently from domain to domain. Three domain types are present: *a*, *b* and *c* (see Fig. 2). The *a* and *b* domains are characterized by oblique grain-boundary alignment and preferred optical orientation with respect to the normal (*N*) to the mylonitic foliation (*Sm*). This obliquity can be described by the α angle (Simpson 1980) which is positive if the preferred orientation is clockwise 'rotated' away from the normal to *Sm* in a sample observed with a dextral sense of shear.

The a *domains*

A foliation at a positive α angle to *N* can be observed in the interior of each *a* domain (Figs. 2 a & b). This foliation is defined by preferred grain-boundary alignment and preferred coincidence of optical orientation. Furthermore neighbouring grains showing the closest coincidence of optical orientation are aligned in a direction with an α angle similar to the α angle of the direction of grain-boundary alignment (Fig. 2 b). This dimensional orientation and spatial distribution of optical coincidence are considered here to be consistent with the sense of shear of the specimen. Such features have been described by Etchecopar (1974), Brunel (1980) and Means (1981), with the same sense of inclination with respect to the mylonitic foliation and lineation.

The c-axes of grains from *a* domains constitute the *a* fabric element in Fig 2(c). The illustration is dextral, so the *a* fabric element is defined by a partial girdle making a positive α angle. When lamellae are present in *a* domains, a single set with traces inclined to the grain boundary alignment direction by approximately 60° is observed. Figure 3 shows the relationships that exist between the lamellae traces and the grain shape in each domain.

The *a* domains and fabric elements are present in all the samples described here from the centres of the shear zones of Cap de Creus. In samples not described here, without a domainal microstructure, the *a* fabric element is also always present.

The b *domains*

The *b* domains are similar to *a* in every respect, and roughly symmetrical about *Sm* so that the α angles of their internal foliation (defined by preferred grain-boundary alignment and preferred optical coincidence direction) are now negative (Figs. 2 a & b). The c-axes from grains belonging to *b* domains define the fabric element *b*, also symmetric to *a* with respect to the *Sm* plane, and thus possessing a negative α angle (Fig. 2c). The traces of the lamellae, when present are inclined to the grain-boundary alignment direction in a similar fashion to *a* domain (Fig. 3).

If it is assumed that a positive α angle shown by the internal foliation and the fabric element is compatible with the sense of shear of the specimen (Etchecopar 1974, 1977, Burg & Laurent 1978, Brunel 1980, Simpson 1980, Means 1981), then *b* grains, domains and fabric elements indicate the opposite sense of shear than that expected in the specimen from field observations.

When the fabric development across a whole shear zone is studied, the presence of *b* grains is shown to depend on the amount of shear deformation undergone by the sample. As shown in recent work with Carreras, with increasing shear strains, the *b* fabric element fades out, while the *a* fabric element maintains its relationships with the foliation (*S* and *Sm*). The fabric symmetry characteristics are determined by the presence or absence of the *b* fabric element (see Figs. 2 c and 8 c & d).

The alternation of *a* with *b* domains give the sample a herring-bone appearance (Figs. 2 a & b). When lamellae are present, they define another herring-bone structure but in the opposite sense (see Figs. 3 and 4).

The c *domains*

The *c* domains consist of equant grains which appear constantly dark between crossed nicols when observed in the direction perpendicular to *Sm* and parallel to *L* (Figs. 2 a & b). The c-axes of *c* grains make up the fabric element labelled *c* in Fig. 2(c). The *c* fabric element consists of a maximum in *Sm* perpendicular to *L* and elongated in the perpendicular plane to *L*. (Fig. 2 c). The grain shape of *c*-grains being equant and the fabric element symmetric with respect to the *Sm* plane they cannot be related to the sense of shear of the specimen. The grains of *c* domains can exhibit two sets of lamellae, the traces of which run parallel to the traces of the lamellae found in *a* and/or *b* domains (Figs. 3 & 4).

RELATIONSHIPS BETWEEN PORPHYROCLASTS AND DOMAINS

Very few quartz porphyroclasts are found in samples displaying a domainal microstructure. They can be divided into three groups: oblate quartz porphyroclasts occupying either *a* or *b* domains; prolate porphyroclasts situated in *c* domains; and very seldom globular porphyroclasts which produce a deflection of the domains. Some feldspar and tourmaline porphyroclasts may be present in the samples.

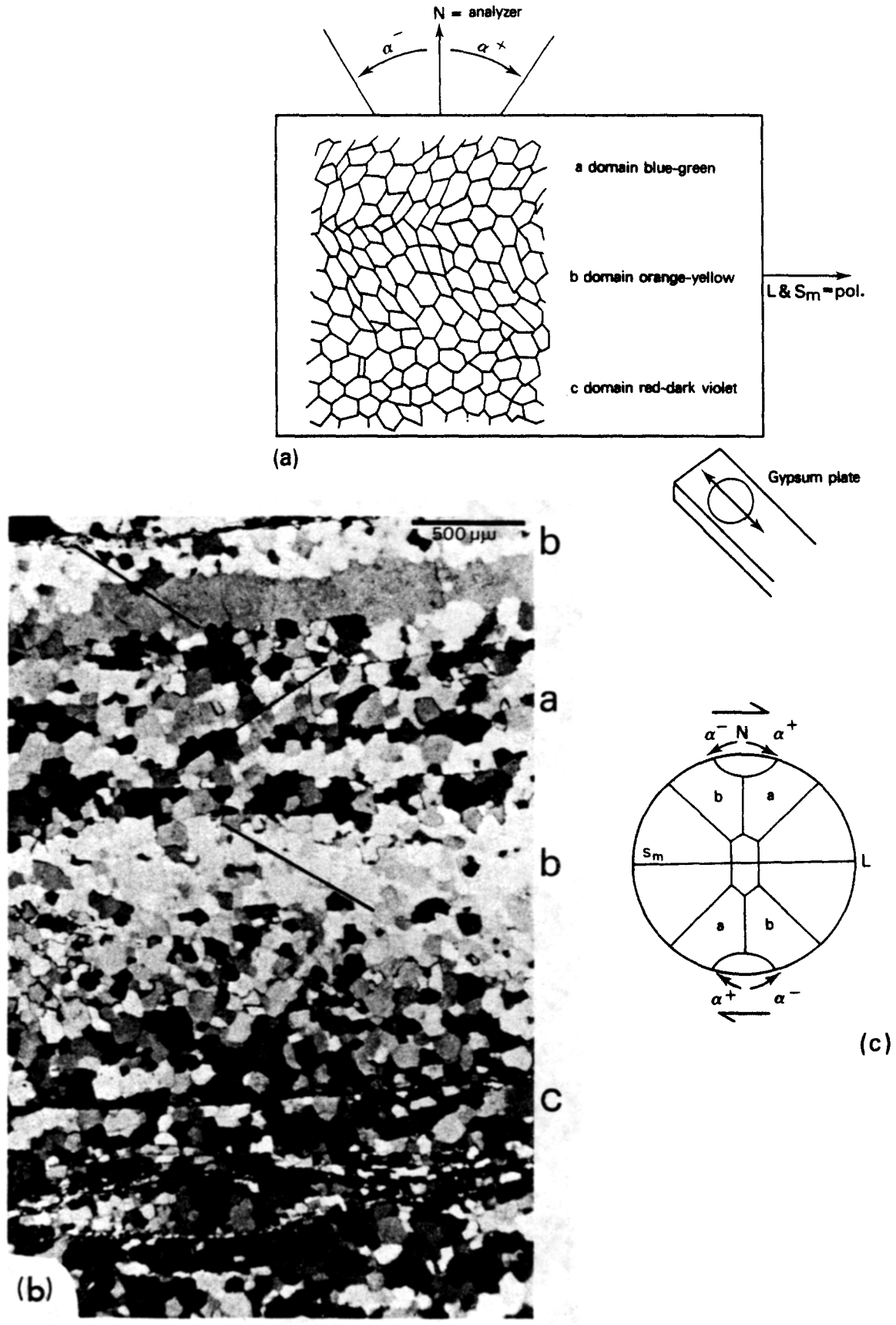

Fig. 2. The domain dispositions with respect to the orientation of S and L. (a) Positive and negative α angles of orientation of grain-boundary alignment with respect to the normal to S (N) are indicated. The interference colours of the domains seen with a gypsum plate are indicated with respect to the orientation of gypsum plate, nicols and S and L for a normal petrographical thin section (30 μm thick). (b) The domain microstructure, same orientation as for (a). Dark lines represent direction of maximum coincidence of optical orientation within a domain. (c) The fabric elements corresponding to the domains. The notation of signs of angles are the same as in (a).

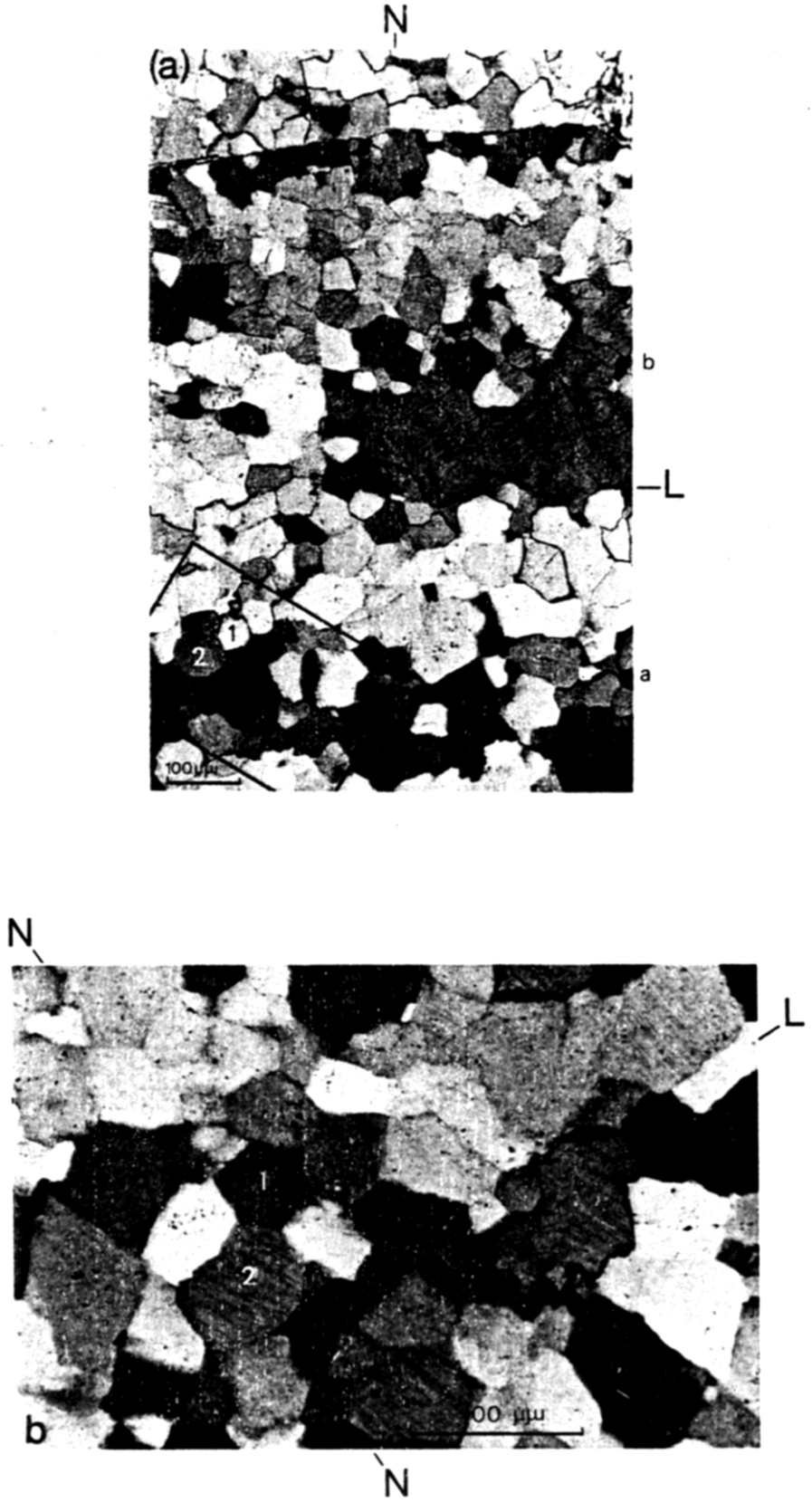

Fig. 3. Relationships between lamellae, domains and remnant oblate quartz porphyroclasts. (a) The old grain remnant belongs to a *b* domain. Top and bottom of the photograph correspond to transitions to *a* domains. Nicols and L and Sm directions are parallel to the edges of the photograph. The position of photograph (b) is outlined together with two numbered quartz grains. (b) Detail of transition to *a* domains. Nicols parallel to the edges of the photograph; N and L are indicated.

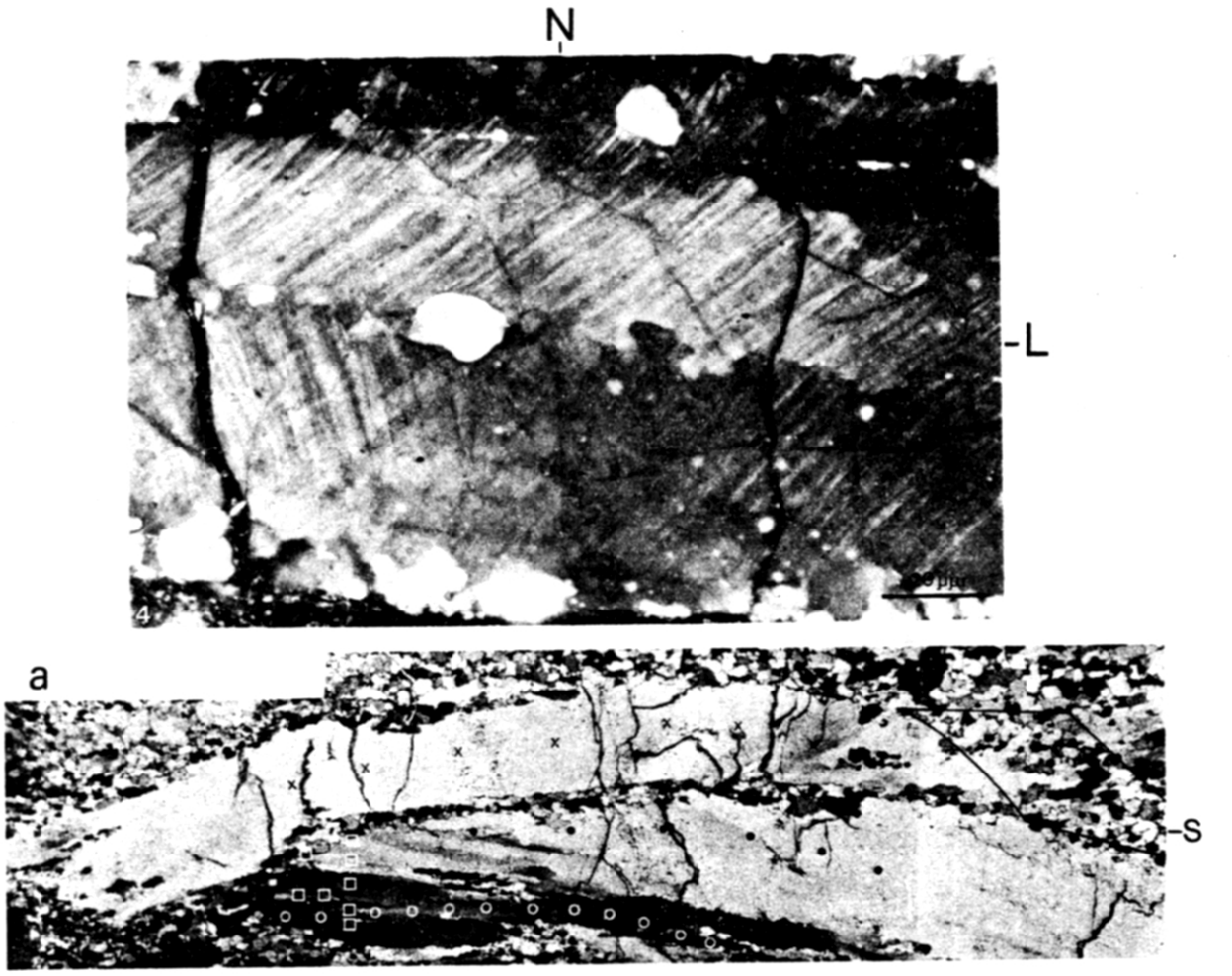

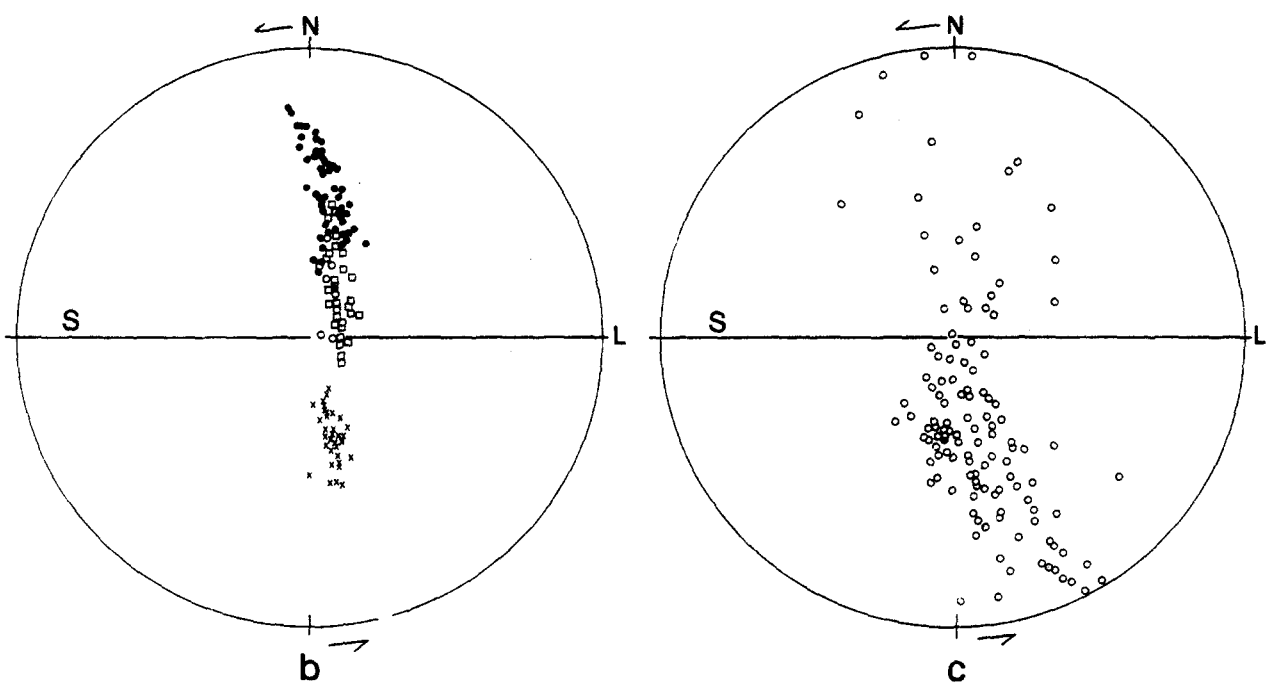

Fig. 4. Lamellae in an elongated quartz porphyroclast. Photomicrograph from a section perpendicular to S. Crossed nicols N and L parallel to photograph boundaries, see text for explanation.

Fig. 5. (a) Photomicrograph of a kinked porphyroclast from a sample from the edges of the mylonite zone (type II sample). Section perpendicular to L; nicols, N and S parallel to the edges of the photograph. (b) c-axes of the different parts of the porphyroclast, symbols correspond to those labelled in the photograph in (a). (c) c-axes of new grains in the top right of the porphyroclast area of measurements outlined.

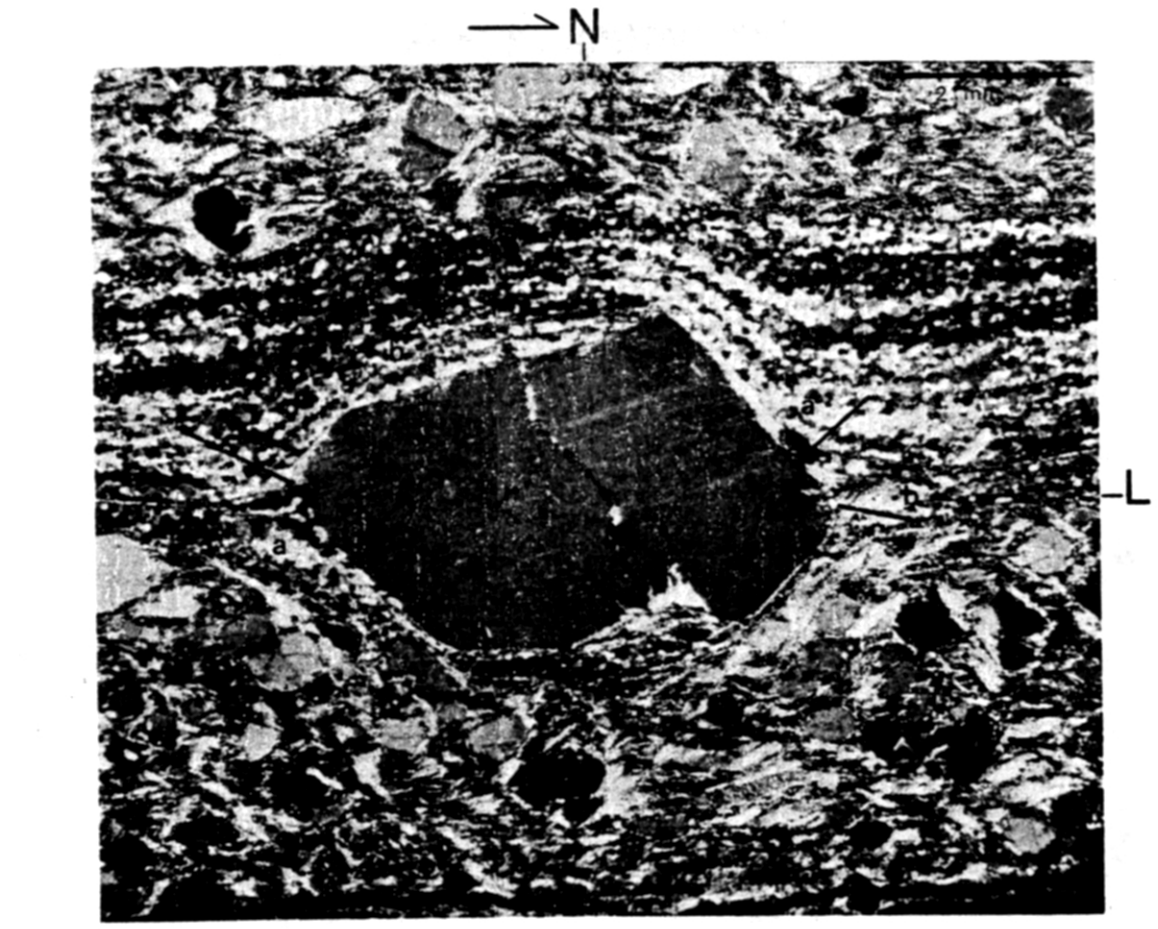

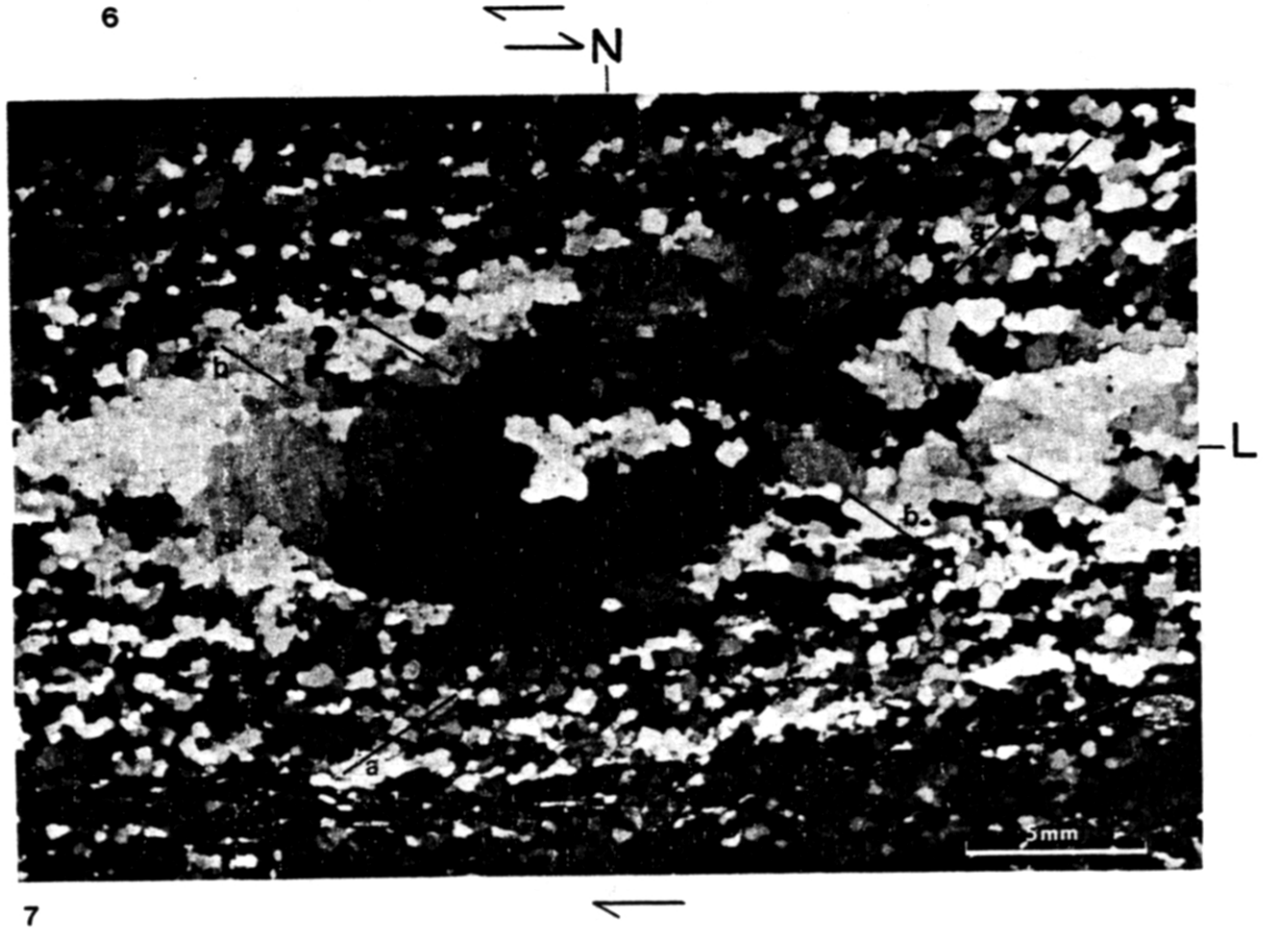

Fig. 6. Wrapping of feldspar porphyroclasts by domains. Explanation in the text. Dark lines represent maximum coincidence of optical orientation. *a* and *b* grains indicated.

Fig. 7. Distortion of microstructures around a globular quartz porphyroclast. Dark lines indicate maximum coincidence of optical orientation.

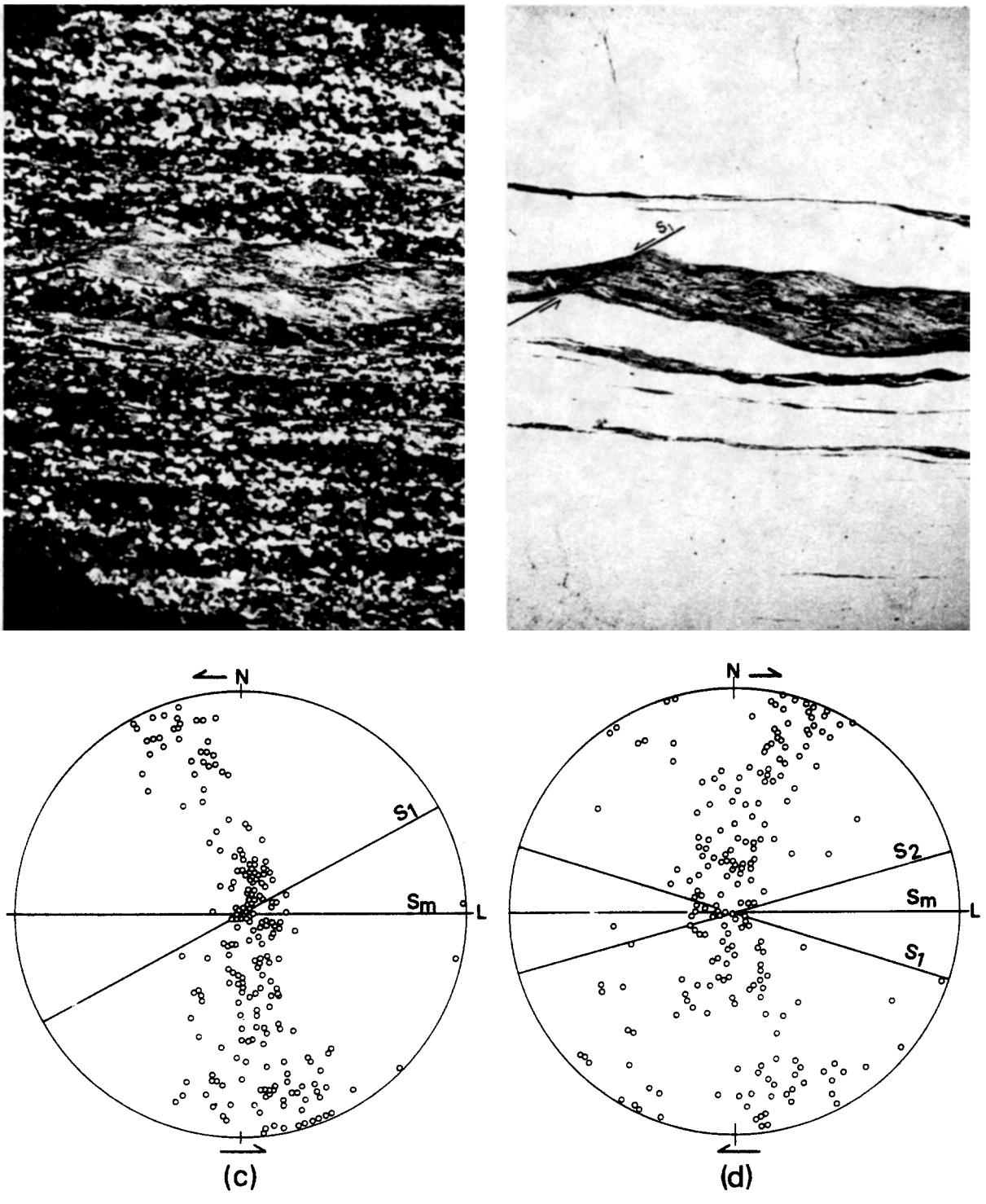

8

Fig. 8. Relationships between crenulations (S_1 and S_2) and domains. (a) Preferred orientation of grains within a domain and its relationship with the crenulation directions. (b) Crenulation axial traces in micas. (c) c-axis fabric from the same specimen. S_1 corresponds to the crenulation trace direction. (d) c-axis fabric crenulation relationship in a symmetric fabric from the centre of a different shear zone. S_1, S_2 are the crenulations, *Sm* is the main mylonitic foliation ($\approx$ X Y plane).

The oblate quartz porphyroclasts

The dimensions of the oblate porphyroclasts are rather variable due to recrystallization; they have long axes which range in length between 1 and 5 mm. Their shape which is oblate (Flinn's $K \approx 0$) in type II samples become less oblate ($0 < K < 1$) in samples of type III. Their boundaries, although serrated, are roughly parallel to the main mylonitic foliation (*Sm*) and are thus parallel to the trend of the domains. Their optical orientation is consistent with the domain in which they are situated. Figure 2(a) shows one porphyroclast of this group positioned in a *b* domain. Figure 3 illustrates how the traces of the lamellae in grains of one domain run approximately parallel for both the porphyroclast and the recrystallized grains.

In samples collected from the edges of the mylonitic bands (type II) which are less deformed than those displaying herring-bone microstructure, oblate porphyroclasts are observed with deformation bands showing different degrees of development. Figure 5 represents such a porphyroclast from a type II sample. The basal plane of the upper part of the porphyroclast is kinked with respect to the middle part (Figs. 5 a & b). The axis of the kink coincides with the direction of the stretching lineation (see Figs. 5 a & b) and the axial plane of the kink corresponds to the foliation plane (*S*). The lower part of the porphyroclast in Fig. 5(a) is rotated with respect to the middle part. The rotation is step-like through successive deformation bands in a fan-like disposition in the left edge of the porphyroclast. In the right side, however, the abrupt change in optical orientation between the middle and lower part of the porphyroclast can again be explained in terms of kinking of the basal plane with an axis similar to that described above (Figs. 5 a & b). The orientation of the subgrains on opposing sides of the kink band boundary again have a herring-bone configuration. Attention has to be paid to the fact that the smaller subgrain boundary orientations are parallel to the directions of maximum optical orientation coincidence in the recrystallized grains. This can be observed in the top right-hand side of the porphyroclast.

The top part of the porphyroclast (shown by crosses in Figs. 5 a & b) cannot be attributed to either an *a* or *b* fabric element; nevertheless, the orientation of the subgrain shapes coincides with the orientation of the new grains in the domain in which it is situated. In this case the new grains belong to the *a* fabric element (see Fig. 5c). Note that the new grain fabric, although related to the porphyroclast orientation, does not follow exactly the trend of spreading of c-axes of the subgrains in the porphyroclast.

The herring-bone microstructure of the domains represented in Figs. 2 and 3 and found in very deformed samples (type III) could be thought of as a further development of the microstructure displayed in Fig. 5, typical of stage II samples.

The prolate porphyroclasts

These porphyroclasts situated in *c* domains, have long axes often greater than 3.5 cm parallel to *L* and they show axial ratios in excess of 70:1. Their c-axes lie near *S* perpendicular to *L*; they thus belong to the *c* fabric element.

Figure 4 shows a part of one of these quartz porphyroclasts. Where lamellae are present, the prolate porphyroclasts present a kink-like appearance. Some parts of these grains appear as kinks because the lamellae bend together across a line, others because of the existence of an additional set of lamellae. However, the basal plane of those crystals is not kinked; in fact, very little variation in their optical orientation is observed across the 'kink boundary', the crystal as a whole plotting in a maximum. The *c* grains can be thought of as the result of polygonization of these prolate porphyroclasts. The lamellae run parallel for both porphyroclasts and recrystallized grains. The dimensional orientation of lamellae traces in *c* domains coincides with the orientation of the lamellae traces of *a* and/or *b* domains. The prolate porphyroclasts as defined here have not been found in type II or I samples.

The rigid porphyroclasts and domain deflection

The domains wrap around rigid porphyroclasts (feldspar, tourmaline and globular quartz porphyroclasts), the curvature of the domains being accompanied by a gradual change in the orientation of the dimensional and c-axis fabric.

Porphyroclasts in the very deformed quartzites and sinistral shear zones in Cap de Creus are rare, and consequently this microstructure has been observed only in dextral shear zones. When an example is observed such that the overall shear is perceived to be dextral, as in Fig. 6, then in the domains wrapping around the feldspar porphyroclast, *a* grains occur at the top right and bottom left sides of the porphyroclast and *b* grains at the bottom right and top left sides. Bouchez (1977) and Mancktelow (1981) describe ribbon porphyroclasts which wrap around globular porphyroclasts. In their photomicrographs, changes in the c-axis orientation in the ribbons can be seen to accompany the bending of the ribbon, and it seems at first sight possible that the change in the domain characteristics around rigid porphyroclasts in Cap de Creus specimens could be explained by polygonization of a ribbon porphyroclast. However, Fig. 7 shows the same domain distribution as Fig. 6 but the deflection of the domains occurs around a globular quartz porphyroclast. The continuity in orientation and shape elongation direction between new grains and subgrains within the globular porphyroclast in Fig. 7 points to a development of the new grains by polygonization of the globular porphyroclast, and the domain distribution could be compared to the tails found in 'cornu' porphyroclasts as described by Etchecopar (1974) and Bouchez (1977).

HERRING-BONE MICROSTRUCTURE SIGNIFICANCE AND ITS RELATIONSHIPS WITH EXTENSIONAL CRENULATIONS

Extensional crenulations are developed in Cap de

Creus shear zones and display a constant angular relationship with the foliation across a shear zone (Carreras & Garcia Celma in preparation).

The relations between fabric elements and crenulation cleavages shown by Ramsauer (in Sander 1950, p. 168) are also found in the Cap de Creus mylonites. In the samples displaying herring-bone microstructure, where micas are present in the thin section, it is observed that the axial traces of two crenulation cleavage sets (S_1, S_2) are nearly perpendicular to the fabric elements *a* and *b*, respectively, as seen in Fig. 8(d). The axial traces of the crenulated micas in the thin section are seen to make a large angle with the preferred grain boundary alignment of the recrystallized grains and the direction of maximum coincidence of optical orientation (Fig. 8 b). For asymmetric fabrics in which the *b* domain is absent, only the set of crenulation cleavages perpendicular to the *a* fabric element is found (Figs. 8a–c). This relationship is also described in Eisbacher (1970, Fig. 7) where the sense of displacement of micas and feldspar clasts is used to determine the sense of shear of the specimen.

DISCUSSION

The herring-bone microstructure seems to develop partially as a result of polygonization of old grains which underwent folding and thereby achieved a final kinked appearance. However attention has to be paid to the fact that in samples of types I and II in which no domainal configuration is present, there is already a considerable percentage of new grains which have orientations quite independent of old grain orientation. In the samples of type III, matrix grains are almost all involved in the domain distribution and it is, thus, also possible that the new grains themselves tend to develop a domainal microstructure. The process by which matrix grains achieve their preferred distribution in domains could be thought of as a relative rotation of areas of matrix grains with respect to each other in the same way as parts of a porphyroclast rotate relatively.

Etchecopar obtained a heterogeneous distribution of cell shapes in his shear simulations (Etchecopar 1974, pp. 117–124). The starting material in his shear simulations was a group of cells of similar polygonal shape and with randomly oriented slip directions in their interiors. The simulation process conserves the area of the cell, and thus the domainal distribution so obtained is not related to any old grain that polygonizes, but due to compatibility constraints on the deformation of neighbouring cells. For pure shear and low intensity simple shear the Etchecopar model produced symmetric fabrics which included cells which had to slip in different senses with respect to the bulk elongation direction for a further deformation increment. These cells can be compared to *a* and *b* grains in terms of their dimensional and crystallographic orientation. A further similarity between Etchecopar's results and the present observations is that asymmetric fabrics consisting only of cells comparable to *a* and *c* grains were produced when the magnitude of simple shear strain was high.

The domain distribution around rigid porphyroclasts seems to reflect differences in the strain conditions. In Fig. 7, for instance, both porphyroclast subgrains and recrystallized grains, pesumably originating from an initially homogeneous crystallographic orientation, acquire different fabrics depending on their position with respect to the inhomogeneity created by the porphyroclast.

The close relationships between the extensional crenulations, the domain distribution and the fabric elements strongly suggests they have developed as the results of the same processes.

The domain characteristics, and their relationships to micas and fabric elements have been described for many places: e.g. the Reintal tectonites (Ramsauer, in Sander 1950), the Austro-Alpine Penninic Nappes (Sander 1950, Brunel 1980), the Cobequid Mylonite zone in Nova Scotia (Eisbacher 1970), the external nappes of the Norwegian Caledonides and the Himalayan Main Central Thrust (Brunel 1980).

Brunel (1980) interpreted the *a* and *c* domain characteristics and their relationships with the fabric diagram, as developing in three stages: firstly, development of the main mylonitic foliation; secondly, shearing in the direction of the elongation of the recrystallized grains and thirdly, reactivation of the main mylonitic foliation. However, in Cap de Creus the domain microstructure, extensional crenulations and fabric characteristics seem to develop together as the result of a single episode of deformation, as postulated by Means (1981). The relationships between those elements is constant across a shear zone, and their orientations in the shear zone are congruent with the schistosity.

Because of the domainal nature of the microstructures described in many sheared quartzites, the warnings of Eisbacher (1970) and Lister & Williams (1980) about the scale, to which microstructural kinematic interpretations apply, should be emphasized. If a thin section is narrower than the width of the domains, or if the fabric measurements are not made in the direction perpendicular to the domain elongation (to the main mylonitic foliation), the measured fabric will vary greatly. Suppose we have a sample composed of the three fabric elements and domains, so that the fabric and microstructure is symmetric with respect to the mylonitic foliation. Such a sample could be collected in a weakly deformed part of a shear zone. A c-axis fabric without maxima perpendicular to *L* is obtained by measuring $a + b$ domains; an asymmetric fabric indicating an opposite sense of shear from the field evidence will be obtained from measuring $b + c$ domains only, or from the top left or bottom right of a rigid porphyroclast. Kinematic deductions about the measured domains could be correct, but should not be applied to the bulk deformation.

CONCLUSIONS

(1) Three types of microstructural and fabric domains

develop in highly deformed quartzites in Cap de Creus shear zones.

(2) The nature of the skeleton of the total c-axis fabric is determined by whether one, two or all three of the different microstructural and fabric domains exist in the measured thin section.

(3) The intensity of maxima in the total c-axis fabric diagrams depends on the relative extent of the different microstructural domains.

(4) As a consequence of (2) and (3), care must be taken when measuring quartz fabrics not to omit any domain; e.g. measuring only $b + c$ domains produces a fabric indicating the wrong sense of shear.

(5) Kinematic deductions are to be applied carefully so as not to surpass the scale for which they are valid; e.g. the sense of shear at certain positions around a competent clast may be opposite to the macroscopic sense of shear.

(6) The new grain elongation, preferred orientation within the domains, and the fabric elements corresponding to *a* and *b* domains define two foliations which have the same significance as the extensive crenulation foliation found in shear zones.

(7) The domains represent distinct strain domains and can develop independently of host grain control.

Acknowledgements—I thank Dr. R. Lisle for invaluable discussions and help during manuscript preparation. Dr. J. Carreras, Dr. G. Lister, Dr. H. Stel and an anonymous referee also contributed to improve the work at different stages.

This work was carried out at the Universities of Barcelona and Utrecht. The author benefited from an exchange scholarship between the Utrecht University and the S.C.I.C. (Consejo Superior de Investigaciones Cientificas) of Spain. Prof. San Miguel and Prof. H. J. Zwart made available all facilities in their respective departments. The work is a part of the unpublished Ph.D thesis of the author.

REFERENCES

Bouchez, J.L. 1977a. Le quartz et la cinematique des zones ductiles. Thesis Doctoral. Université de Nantes.

Bouchez, J.L. 1977b. Plastic deformation of quartzites at low temperature in an area of natural gradient. *Tectonophysics* **39**, 25–50.

Brunel, M. 1980. Quartz fabrics in shear zone mylonites: evidence for major imprint due to late strain increments. *Tectonophysics* **64**, T33–T44.

Burg, J.P. & Laurent, Ph. 1978. Strain analysis of a shear zone in a granodiorite. *Tectonophysics* **47**, 15–42.

Carreras, J. 1973. Petrologia y análisis estructural de las rocas metamórficas en la zona del Cabo de Creus (Provincia de Gerona). Thesis Doctoral (unpublished). Universidad de Barcelona.

Carreras, J. 1974. Progressive mylonitization in quartzitic and quarzofeldspathic rocks in the belts of the Cap de Creus (E. Pyrenees, Spain). M.Sc. thesis (unpublished). Imperial College London.

Carreras, J. 1975a. Determinación de las relaciones angulares y de la deformación por cizalla, para cizallamientos en materiales con una heterogeneidad planar. *Acta geologica hispán.* **10**, 141–145.

Carreras, J. 1975b. Las deformaciones tardi-hercínicas en el litoral septentrional de la península del Cabo de Creus (prov. de Gerona, Espana); la génesis de las bandas miloníticas. *Acta geologica hispán.* **10**, 109–115.

Carreras, J. & Santanach, P.F. 1973. Micropliegues y movimientos en los cizallamientos profundos del Cabo de Creus (prov. Gerona, Espana). *Est. Geol.* **29**, 439–450.

Carreras, J., Estrada A. & White, S. 1977. The effects of folding on the c-axis fabrics of a quartz mylonite. *Tectonophysics* **39**, 3–24.

Eisbacher, G.H. 1970. Deformation mechanics of mylonitic rocks and fractured granites in Cobequid Mountains, Nova Scotia, Canada. *Bull. geol. Soc. Am.* **81**, 2009–2020.

Etchecopar, A. 1974. Simulation par ordinateur de la deformation progressive d'un agregat polycristallin. Thesis Doctoral, Université de Nantes, France.

Etchecopar, A. 1977. A plane kinematic model of progressive deformation in a polycrystalline aggregate. *Tectonophysics* **39**, 121–139.

Lister, G.A. & Price, G.P. 1978. Fabric development in a quartz–feldspar mylonite. *Tectonophysics* **49**, 37–78.

Lister, G.S. & Williams, P.F. 1980. Fabric development in shear zones: theoretical controls and observed phenomena. *J. Struct. Geol.* **1**, 283–297.

Mancktelow, N.S. 1981. Strain variation between quartz grains of different crystallographic orientation in a naturally deformed metasiltstone. *Tectonophysics* **78**, 73–84.

Means, W.D. 1981. The concept of steady-state foliation. *Tectonophysics* **78**, 179–199.

Sander, B. 1950. *Einführung in die Gefügekunde der geologischen Körper*. Springer, Wien.

Simpson, C. 1980. Oblique girdle orientation patterns of quartz c-axes from a shear zone in the basement core of the Maggia Nappe. Ticcino. Switzerland. *J. Struct. Geol.* **2**, 143–170.

White, S. 1976. The effects of strain on the microstructures, fabrics and deformation mechanisms in quartzites. *Phil. Trans. R. Soc. Lond.* **A283**, 69–86.